

ON FLOW REVERSAL BOUNDARIES AND TRANSPOLAR VOLTAGE IN AVERAGE MODELS OF HIGH-LATITUDE CONVECTION

MIKE LOCKWOOD*

Rutherford Appleton Laboratory, Chilton, Didcot, Oxon OX11 0QX, U.K.

(Received in final form 30 July 1990)

Abstract—The implications of polar cap expansions, contractions and movements for empirical models of high-latitude plasma convection are examined. Some of these models have been generated by directly averaging flow measurements from large numbers of satellite passes or radar scans; others have employed more complex means to combine data taken at different times into large-scale patterns of flow. In all cases, the models have implicitly adopted the assumption that the polar cap is in steady state: they have all characterized the ionospheric flow in terms of the prevailing conditions (e.g. the interplanetary magnetic field and/or some index of terrestrial magnetic activity) without allowance for their history. On long enough time scales, the polar cap is indeed in steady state but on time scales shorter than a few hours it is not and can oscillate in size and position. As a result, the method used to combine the data can influence the nature of the convection reversal boundary and the transpolar voltage in the derived model. This paper discusses a variety of effects due to time-dependence in relation to some ionospheric convection models which are widely applied. The effects are shown to be varied and to depend upon the procedure adopted to compile the model.

INTRODUCTION

Various empirical models of high-latitude ionospheric plasma convection have been produced, using data either from low-altitude polar-orbiting satellites (Heppner, 1977; Volland, 1978; Heelis *et al.*, 1982; Heppner and Maynard, 1987; Rich and Maynard, 1989; Lu *et al.*, 1989; Hairston and Heelis, 1990) or from ground-based radars (Foster, 1983; Oliver *et al.*, 1983; Holt *et al.*, 1987; Etemadi *et al.*, 1988). Equivalent convection patterns have been derived from magnetometer data using models for the spatial distribution of ionospheric conductivities (e.g. Friis-Christiansen *et al.*, 1985). Quantitative models of the pattern of ionospheric convection are often used in numerical simulations of the coupled ionosphere–thermosphere system for which they describe energy and momentum input from the magnetosphere as well as inducing important effects by transporting plasma between regions where different production/loss and heating/cooling processes are effective [see reviews by Rees and Fuller-Rowell (1989) and Sojka (1989)]. Several studies have combined simultaneous measurements from a number of observatories to produce “snapshots” of the flow pattern (Richmond *et al.*, 1988; Foster *et al.*, 1989), but this has only been

possible for limited periods of intensive study. In general, the convection models have been generated by combining large numbers of satellite passes or radar scans. Such convection models are implicitly steady state as it assumed that for a given set of controlling parameters [for example the Interplanetary Magnetic Field (IMF) and/or some index of terrestrial magnetic activity] the flow pattern has a given form, independent of its history prior to that time, and data from different satellite passes/radar scans can be combined. Recently, Rostoker *et al.* (1988) and Hapgood *et al.* (1991) have estimated from the observed variability of the IMF that the ionosphere/magnetosphere system could be in steady state for at most 15% of the time and that even for much of that time the convection pattern may not be in genuine steady state but undergoing regular oscillations. Hence departures from steady state must be considered the norm, rather than relatively infrequent events. Lockwood *et al.* (1990) have discussed responses of convective flows and the corresponding current systems to changes in the IMF and conclude that the convection pattern must be considered as the sum of two intrinsically time-dependent patterns, rather than a single steady-state pattern.

The steady-state empirical models have, however, been exceptionally valuable in the study of the coupled magnetosphere–ionosphere–thermosphere system, and the purpose of this paper is not to question most of the knowledge and understanding which has

* Also Visiting Honorary Lecturer, Blackett Laboratory, Imperial College, London SW7 2BZ, U.K.

derived from them. Rather it attempts to define limitations to their use and warn against applications which go beyond those intended by their constructors. In particular, the relationships of convection models to the various mechanisms thought to be responsible for the excitation of ionospheric convection are evaluated. A companion paper (Lockwood *et al.*, 1991) will address the implications for modelling of the ionosphere-thermosphere system during non-steady conditions. However, this paper does not go into each application in detail, but aims to establish some general principles. In the conclusions, some ways that models could be generalized from steady state are briefly explored.

IONOSPHERIC FLOW REVERSALS AND MAGNETOPAUSE MOMENTUM TRANSFER MECHANISMS

In all convection patterns, there are flow reversals between the generally antisunward flows of the convection polar cap, and the generally sunward flows of the auroral oval. In satellite data, this convection reversal boundary has two forms, showing either "shear" or "rotational" flow reversals. Shear reversals are generally found nearer dawn and dusk, whereas rotational reversals are nearer noon and midnight (Heelis *et al.*, 1976, 1982; Heelis and Hanson, 1980; Heelis, 1984). Radar data, on the other hand, have tended to show rotational reversals: for example, Jørgenson *et al.* (1984) found rotational reversals throughout the dayside. However, these incoherent scatter radar observations usually employ some form of the beamswinging technique and the inherent assumptions about the spatial uniformity of the flow will tend to cause derived vectors to rotate in the presence of real flow shears (Lockwood *et al.*, 1988). The average convection models also do not generally show shear reversals (Heppner and Maynard, 1987; Holt *et al.*, 1987). In fact, the only model which does [that due to Heelis *et al.* (1982)] was designed specifically to allow the maintenance of the shear flow boundaries observed in the satellite data and avoided averaging data, which would tend to smooth out such shears. It is interesting to note here that shear and rotational reversals can only be uniquely distinguished in data from a single satellite pass by considering both field-perpendicular flow components—i.e. both along and perpendicular to the satellite path. In compiling their model, Heppner and Maynard (1987), only had available the component perpendicular to the orbit (giving the distribution to electric potential along the orbit). The nature of the reversal is then derived by comparing the dis-

tributions of potential for orbits which cut the convection reversal boundary at different magnetic local times (M.L.T.). Figure 1 demonstrates some of the differences between models by contrasting a Heelis *et al.* model flow pattern with one of the Heppner and Maynard models: both are shown in a M.L.T.-invariant latitude (Λ) frame co-rotating with the Earth. Part (a) shows the Heppner and Maynard "A" model (for IMF B_z positive/negative in the Southern/Northern Hemisphere) and part (b) shows the best fit Heelis *et al.* model to the pattern shown in (a) [from the work of Rich and Maynard (1989)].

There are a number of differences between the two patterns shown in Fig. 1, but we wish here to concentrate on the nature of the dayside flow reversals or, equivalently, on the distribution of potential around the dayside convection boundary reversal, because that has particular implications for (1) how convection is excited by the interaction of the solar wind flow with the terrestrial magnetosphere and (2) how plasma densities evolve as flux tubes are moved around the high-latitude F -region. In the Heelis *et al.* model there are longer segments of equipotential boundary (i.e. shear reversals) between segments of rotational flow reversal (into the polar cap on the dayside and out of it on the nightside). This model is particularly easy to interpret in terms of convection driven by magnetic reconnection. The rotational reversal on the dayside is then taken to map to the reconnection X -line on the dayside magnetopause, whereas that on the nightside maps to the X -line in the geomagnetic tail. The voltages along the reconnection X -lines are mapped down the magnetic field lines and applied across the regions of rotational reversal or "merging gaps". Because these two reconnection X -lines are unlikely to be contiguous, it is expected that there are segments of equipotential boundary between them (shear flow reversals). From satellite data, various authors have argued that the dayside merging gap is narrow (the so-called convection "throat") (Reiff *et al.*, 1978; Heelis, 1984; Burch *et al.*, 1985). However, others have found that the regions of rotational reversal are not narrow and extend throughout the dayside (Jørgensen *et al.*, 1984). Of relevance to this difference between the two models is a statistical survey of trans-auroral voltage by Lu *et al.* (1989). They found that the measured potential at the polar cap boundary could generally be fitted with a sinusoidal function of M.L.T., although for some IMF orientations there was significant evidence for a more restricted throat than given by this simple function of M.L.T. Generally, however, the survey of Lu *et al.* supported the rotational reversals throughout the dayside found in

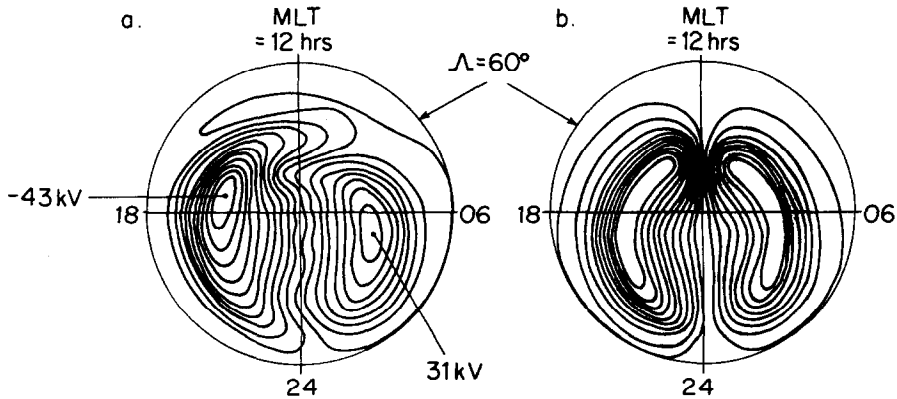


FIG. 1. EMPIRICAL HIGH-LATITUDE CONVECTION MODELS.

(a) The “A” model of Heppner and Maynard (1987)—one of their two models for IMF $B_y < 0$ in the Northern Hemisphere and $B_y > 0$ in the Southern Hemisphere. (b) Best fit Heelis *et al.* (1982) model to the pattern shown in (a) (as fitted by Rich and Maynard, 1989). Contours of electric potential are shown 4 kV apart and the transpolar voltage Φ_{pc} is 74 kV.

the Heppner and Maynard model (although, as we shall show, the voltages along segments of the boundary away from noon were not as great as in the Heppner and Maynard model). Another recent model by Hairston and Heelis (1990) also provides some evidence for a throat, but again shows rotational reversals throughout the dayside. Such extended rotational flow reversals are often interpreted in terms of the other process thought to contribute to the excitation of magnetospheric and ionospheric convection, namely “viscous-like interaction” (see e.g. Foster, 1983). This is because, whereas a narrow throat configuration is well explained by the reconnection model, the viscous-like interaction might be expected to act throughout the dayside. However, in the reconnection model, the extent of the magnetopause X -line and the possible distribution of reconnection rate along that X -line are not known, nor is the mapping of magnetic field lines from the magnetopause to the dayside polar cap boundary. As a result, the shape of the dayside ionospheric flow pattern (in particular the occurrence of rotational and shear flow reversals) does not unambiguously distinguish between the two types of momentum transfer across the magnetopause. A further complication is the fact that there are several reversals in some flow data (as reflected in some models, for example Fig. 1a) and different choices as to which is the polar cap boundary radically alters the derived voltage distribution (see Cowley *et al.*, 1991).

From observations of the dawn-to-dusk transpolar voltage, Φ_{pc} , as a function of IMF orientation, it is thought that reconnection generates a total voltage of up to about 100 kV across the polar cap, depending

upon the magnitude of the southward component of the IMF (i.e. negative B_z) (Reiff *et al.*, 1981; Doyle and Burke, 1983; Wygant *et al.*, 1983; Cowley, 1984; Reiff and Luhmann, 1986). However, a roughly constant value (i.e. independent of B_z) of up to 30 kV is observed when the IMF is northward and this is often attributed to the viscous-like interaction. Lockwood *et al.* (1990) have recently pointed out that a significant part of this voltage could be due to continuing reconnection in the geomagnetic tail, consistent with the decay in transpolar voltage observed by Wygant *et al.* (1983) following northward turnings of the IMF. Somewhat lower values for the voltage due to viscous-like interaction (< 20 kV) have been inferred from the voltage across the low-latitude boundary layer at the magnetopause (Mozer, 1984) and the flow across the dawn polar cap boundary (Lockwood *et al.*, 1988), consistent with the Φ_{pc} observed after prolonged periods of northward IMF (Wygant *et al.*, 1983).

In order to quantify the differences between the two models shown in Fig. 1, it is useful to compute the voltage along two 4-h segments of the convection reversal boundary: Δ_m is the voltage across the 06:00–10:00 M.L.T. (morning) segment and Δ_a is the voltage across the 14:00–18:00 M.L.T. (afternoon) segment. For the form of the Heelis *et al.* model shown, these segments are equipotential ($\Delta_m = \Delta_a = 0$), whereas in the Heppner and Maynard “A” model there is a voltage of roughly 24 kV placed across the afternoon segment and about 20 kV across the morning segment ($\Delta_m = 20$ kV, $\Delta_a = 24$ kV), for a total transpolar voltage, Φ_{pc} , of 74 kV. If the ionospheric projection of the magnetopause X -line extends before 10:00 M.L.T.

and/or after 14:00 M.L.T., reconnection could contribute to Δ_m and/or Δ_a . We do not know the length of this merging gap. However, we note another ionospheric signature, thought to be closely associated with dayside reconnection, is cusp particle precipitation (see Reiff *et al.*, 1977), which typically covers ~ 2 h of M.L.T. within the segment 10:00–14:00 M.L.T. (Newell and Meng, 1989). On this basis we would not expect reconnection to contribute to either Δ_m or Δ_a , which would normally, therefore, be thought to result from viscous-like interactions. However, the sum of Δ_a and Δ_m is 44 kV for the Heppner and Maynard models, somewhat larger (by a factor of about 2) than we would expect due to viscous-like interaction at the flanks of the magnetopause (from the discussion and references given above, the total expected contribution to Φ_{pc} should be at most 20 kV). The sinusoidal variations in boundary potential fitted by Lu *et al.* give $(\Delta_m + \Delta_a) \approx 37$ kV for this Φ_{pc} of 74 kV, which is slightly more consistent with, but still considerably greater than, the potential expected for viscous-like interaction. Lockwood *et al.* (1988) observed flow into the polar cap corresponding to 7 kV between 06:00 and 08:00 M.L.T. If this flow speed were constant for 06:00–10:00 and 14:00–18:00 M.L.T., this would give $(\Delta_m + \Delta_a)$ of 28 kV; again this is lower than for the Heppner and Maynard model. However, two points should be noted here: first, these radar data are for just 2 h in 1 day and may well therefore not be typical. Secondly, the voltage across the 08:00–10:00 M.L.T. and 14:00–16:00 M.L.T. segments may be greater than that observed over 06:00–08:00 M.L.T. (and assumed to apply for 16:00–18:00 M.L.T.): hence the Lockwood *et al.* radar result could be consistent with the Heppner and Maynard model values for Δ_m and Δ_a .

It is known that the polar cap, as defined from particle precipitation, expands and contracts in response to changes in reconnection rate at the dayside magnetopause and in the geomagnetic tail (Holzer *et al.*, 1986). The convection reversal boundary has been shown to similarly move equatorward and poleward (Lockwood *et al.*, 1986b, 1988; de la Beaujardiere *et al.*, 1987). Satellite observations show that the convection polar cap is not only variable in size (depending upon the solar wind, IMF and geomagnetic activity), but is also shifted in the Y direction, depending on the IMF B_y component (Heppner, 1972, 1973, 1977; Mozer *et al.*, 1974; Hairston and Heelis, 1990). These shifts, and those depending upon the IMF B_x component [recently discussed by Cowley *et al.* (1991)], are reflected in average convection models (Holt *et al.*, 1987; Heppner and Maynard, 1987). In this paper, we will discuss how these

motions in the location of the convection boundary reversal can affect the nature of the reversal and possibly produce rotational flow features, suggestive of viscous-like interaction, in both instantaneous flow snapshots and average convection models. We quantify these effects by estimating their contribution to the voltages Δ_m and Δ_a .

CONVECTION REVERSALS IN AVERAGED FLOW DATA

Figure 2 shows a shear reversal at the point Q , but a rotational reversal at P . If this convection boundary moves, averaging will cause a decrease in average flow speeds parallel to the boundary. This is because at any point over which the boundary moves, flows will have opposite directions depending on where the boundary is relative to that point. Etemadi *et al.* (1988) did find that mean flow speeds decreased near the convection boundary. However, Todd *et al.* (1988) and Lockwood *et al.* (1988) noted the same feature could also be observed in case studies of radar data, and Lockwood *et al.* showed this could, at least in part, be generated by the effect of the radar beamswinging technique in the presence of a shear boundary. On the other hand, there will be no spurious flows normal to

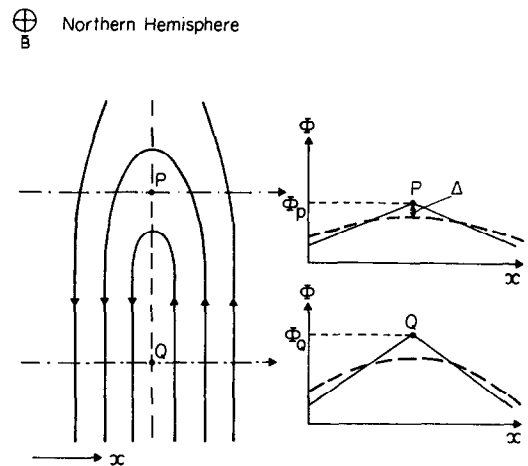


FIG. 2. THE CONVECTION REVERSAL BOUNDARY. The points P and Q are intersections of satellite paths (dot-dash lines) with the convection reversal boundary (dashed line): P is a flow rotational reversal and Q a shear reversal, as shown by the streamlines (solid lines). In most models, rotational reversals between P and Q do not arise because of measured flows across the boundary, but rather because the potential at P is lower than at Q , as shown by the along-orbit distributions of electric potential shown on the right: the solid lines are for an instantaneous flow snapshot, the dashed lines are means when there is variability in the location of the boundary at P and Q .

the boundary introduced by the averaging procedure (although Lockwood *et al.* showed that such spurious flows could be generated by the radar beamswinging technique). For example, for a perfect shear this component will be constant along a satellite orbit (for a constant orientation of the boundary with respect to that orbit) and hence the average is the same as the instantaneous values. Therefore a mean model which was synthesized with great weight given to the mean boundary normal flow component would not show any spurious flows into the polar cap caused by averaging over periods when the boundary was in motion.

However, several flow models from satellite data were not compiled using two components of the flows, but only the flow perpendicular to the satellite orbit (i.e. the electric field along the satellite orbit) (e.g. Heppner, 1977; Volland, 1978; Heppner and Maynard, 1987; Lu *et al.*, 1989). In Fig. 2 we consider two satellite passes normal to the boundary. In general, satellite passes will not be orthogonal to the boundary, but the generally East–West orientation of the boundary, with the generally North–South orientation of the satellite passes, means that the angle between the two is usually quite large and the conclusions drawn here do not depend upon orthogonality. The left hand of the figure shows the potential distribution along these two orbits. If the peak potential at P is lower than that at Q , fitted equipotentials must cross the boundary between P and Q , as shown on the left-hand side of Fig. 2. In the Heppner and Maynard model, the rotational reversals arise in this way, because the mean potential at P is found to be different from that at Q .

As discussed above, boundary motions will cause an apparent slowing of the flow at the boundary for models obtained by purely arithmetic averaging of data from many satellite orbits. The dashed lines in the along-orbit potential distributions shown on the right of Fig. 1 show the mean values from many passes when there is variability of the locations of P and Q . It can be seen that, because of the averaging process, the variability in the boundary location has reduced the peak potential at the mean locations of P and Q , compared with its value for each individual case. Therefore, if we always had a shear flow reversal (i.e. P and Q were at the same potential at all times) but there was greater variability of the boundary latitude at the M.L.T. of P than at the M.L.T. of Q , the average of the potential magnitude at P would be lower than that at Q and the average models would show rotational flow into the polar cap between P and Q , which was not actually present at any time.

Hence if averaging is done this way, oscillations in shape in the polar cap can produce apparent

rotational reversals in mean flow models. In particular, if the latitude of the polar cap were more variable at noon than at dawn and dusk, a spurious rotational reversal could be introduced throughout the dayside in this type of averaged model. Such variability is exactly as expected if the polar cap shows the effects of magnetospheric erosion (i.e. the noon polar cap boundary moves rapidly equatorward in response to enhanced reconnection) and then relaxes back poleward as the polar cap recovers its more circular form. The ionospheric effects of erosion are seen in the latitudinal position of the cusp precipitation (Burch, 1973) and in ionospheric flow patterns (Freeman and Southwood, 1988).

In order to quantify the possible effect of averaging and boundary variability, consider that at the M.L.T. of P , the boundary latitude has a Gaussian distribution of standard deviation 3° , whereas at Q the boundary does not vary in latitude but is otherwise the same as at P . At any instant of time P and Q are at the same potential ($\Phi_P = \Phi_Q$) and hence the boundary PQ is always an equipotential contour (i.e. a shear flow reversal). If Q is at dawn and P at 10:00 M.L.T., the reduction in the peak of the mean potential at the M.L.T. of P , Δ , caused by the averaging, will equal Δ_m in the averaged convection model. Similarly, for Q at dusk and P at 14:00 M.L.T., the increase in the minimum potential at the M.L.T. of P , $\Delta = \Delta_a$. By averaging, we find the mean potential at the mean location of P is:

$$\langle \Phi_P \rangle = \Phi_P - \Delta = \Phi_P - v_p B \sigma \sqrt{(2/\pi)}, \quad (1)$$

where v_p is the convection speed parallel to the boundary, B is the ionospheric magnetic field and σ is the standard deviation of the boundary location (taken here to be 330 km, equivalent to 3° of latitude). For typical convection speeds, v_p , of 1 km s^{-1} we find Δ is 13 kV.

This effect will be present if the cross-orbit flow (along-orbit electric field) data are averaged and the location and potential of a point on the convection boundary then derived from the along-track distribution of the mean potential. A similar effect will be present if radar flow data for a given location are averaged together; however, the effect will be harder to predict because equipotential contour fitting will, to some extent, also be influenced by the mean observed flow speeds normal to the boundary. It appears that Heppner and Maynard have avoided this effect completely by scaling off the latitude and potential and averaging these two parameters separately. In the above example, $\langle \Phi_P \rangle = \Phi_P$ for their procedure and hence Δ is zero.

In the foregoing, we have considered the variability of the latitude of the dayside convection boundary. As pointed out by Lu *et al.* (1989), a second effect could be the variability of the M.L.T. of the dayside rotational reversal region. This would influence all average models, including that of Heppner and Maynard. Consider 10:00–14:00 M.L.T. to be the mean positions of the ends of the merging gap, as in the Heelis *et al.* model, but that there is variability about these means. If the merging gap at any instant extends, for example, a distance d to the East of 14:00 M.L.T. there will be a voltage drop of $\delta = v_n B d$ to the East of 14:00 M.L.T., where v_n is the northward flow speed in the merging gap. If the standard deviation of d is σ , on averaging we find

$$\Delta_m = \langle \delta \rangle = v_n B \sigma / \sqrt{(2\pi)}. \quad (2)$$

For $v_n = 750 \text{ m s}^{-1}$ (equivalent to a voltage of roughly 100 kV across a 4-h merging gap) and $\sigma = 650 \text{ km}$ (equivalent to roughly 1 h of M.L.T.), we find that $\Delta_m = \Delta_a = 10 \text{ kV}$.

DEPARTURES FROM STEADY STATE

We shall here define the polar cap to be the region of open flux tubes. We will consider only flows driven by reconnection, in which case the convection reversal boundary and the polar cap boundary will coincide. This is not to say that there are not other processes which act to drive convection, i.e. the “viscous-like interactions” we discussed in the Introduction. However, by considering departures from steady state, we discuss how ionospheric flow observations could, to some extent, mimic the effects of viscous-like interaction, even when only reconnection-driven flows are present and the dayside merging gap is narrow.

In Fig. 3, we show four ways in which the polar cap can depart from steady state. In (a) the polar cap is expanding because of an imbalance between dayside and nightside reconnection rates: in this case the rate at which field lines are opened at the dayside magnetopause exceeds that at which they are closed in the geomagnetic tail on the nightside and hence the polar cap expands. In part (b), the polar cap is contracting because reconnection on the nightside proceeds faster than that on the dayside. The flow patterns shown were sketched by Lockwood and Freeman (1989) and are generalizations of the modelling by Siscoe and Huang (1985). Moses *et al.* (1989) have calculated flow patterns for this expanding/contracting polar cap model during substorms and found the results compared favourably with data from selected satellite passes. Lockwood *et al.* (1990) have discussed how

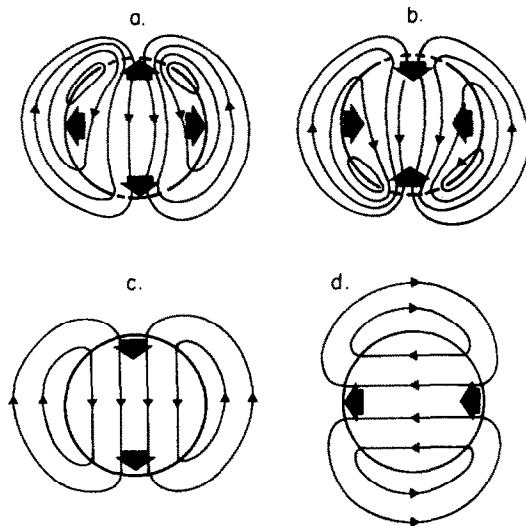


FIG. 3. DEPARTURES FROM STEADY STATE OF THE POLAR CAP. (a) Shows the flows for an expanding polar cap, and (b) is for a contracting polar cap (after Lockwood and Freeman, 1989). The flows caused by anti-sunward and duskward motions of the cap as a whole are shown in (c) and (d) (after Southwood, 1987). Thin lines are plasma flow streamlines, dashed lines are the “merging gaps” (mapping to reconnection X -lines) and heavy solid lines are adiaroic polar cap boundaries. Solid arrows denote the direction of boundary motions.

this model can explain the observed response delays of ionospheric flows to changes in the IMF and how it is also consistent with previous observations of the behaviour of high-latitude ionospheric current systems. The rates of flux transfer into and out of the polar cap are quantified by Φ'_d and Φ'_n which are the voltages along the reconnection X -lines, which equal the voltages along the corresponding ionospheric projections of those X -lines in their own rest frame. By our definition of the polar cap, these projections are segments of the polar cap boundary and we here term them “merging gaps” and show them as dashed lines in Fig. 3. The remaining segments of the polar cap boundary (solid lines) are termed “adiaroic” (meaning “not flowing across”) after Siscoe and Huang. de la Beaujardiere *et al.* (1987) considered radar observations of a dayside convection boundary at 14:00 M.L.T. and concluded that it was not adiaroic as it moved equatorward while plasma flows near it were poleward. This analysis assumed that the cap boundary was aligned with the L -shell and large errors can be introduced by this assumption because of the large magnitudes of flows parallel to the boundary, although the conclusions are unlikely to be altered in this case.

On the other hand, examples of moving adiaroic boundaries have been observed. Lockwood *et al.* (1988) studied an example near dawn and were able to determine the boundary orientation from the measured ion temperatures at the two radar beams used and hence showed that the boundary motion and the boundary-normal component of the local plasma flow were very similar. Therefore, although there was some viscous-like interaction, the convection reversal boundary was very close to being an adiaroic polar cap boundary. This example occurred during a major polar cap contraction (Clauer *et al.*, 1989), and the boundary is of the kind shown in Fig. 3b. In another case, Lockwood *et al.* (1986b) observed an adiaroic polar cap boundary at 14:00 M.L.T. during multi-radar and satellite observations of a major polar cap expansion: this is an example of the situation sketched in Fig. 3a. Note that in the sketched flow patterns, the polar cap is assumed to remain circular in which case the difference between Φ'_d and Φ'_n is distributed uniformly along the entire polar cap boundary. As this includes the merging gaps, the voltages across them in the frame of reference fixed with respect to the Earth, Φ_d and Φ_n , are somewhat different from Φ'_d and Φ'_n . As discussed by Lockwood *et al.* (1990), for a circular polar cap, we can write:

$$\Phi_d - \Phi_n = (\Phi'_d - \Phi'_n)(1 - f), \quad (3)$$

where f is the fraction of the polar cap boundary made up by the two merging gaps (i.e. a fraction $1 - f$ of the boundary is adiaroic). The differences between the voltages in the rest frame of the merging gaps and in the Earth's frame can be increased by shape changes in the polar cap which cause additional movement of the merging gaps—for example “erosion” on the dayside (Freeman and Southwood, 1988) or any “poleward leap” on the nightside (Hones, 1985).

Generally, the polar cap area, A , is governed by Faraday's law (e.g. Lockwood and Freeman, 1989)—equivalent here to a law of conservation of open magnetic flux:

$$(\Phi'_d - \Phi'_n) = B(dA/dt), \quad (4)$$

where B is the ionospheric magnetic field strength. For a circular polar cap, equations (3) and (4) yield

$$(\Phi_d - \Phi_n) = (1 - f)B(dA/dt). \quad (5)$$

Parts (c) and (d) of Fig. 3 show the effects of translational motion of the polar cap: in part (c), the polar cap as a whole is moving anti-sunward (in the $-X$ direction, i.e. $V_x < 0$) and in (d) it is moving duskward at speed V_y . The flow patterns are as given by Southwood (1985, 1987) for circular FTE flux tubes. The situation in (c) could be caused by a change in the B_x

component of the IMF, via magnetic tension (Cowley *et al.*, 1991). However, it is much more likely to result from a complex combination of the merging rate imbalances and recovery from erosion and/or a poleward leap, as discussed above. The motion shown in (d) would be expected following changes in the Y component of the IMF, due to the effects of magnetic tension (see Cowley, 1981; Cowley *et al.*, 1991). Such shifts in the polar cap in the Y direction have been observed in convection patterns (Heppner, 1972, 1973; Mozer *et al.*, 1974), consequent magnetic disturbances at the ground (e.g. Friis-Christensen *et al.*, 1985) and in the location of aurorae (Meng, 1980; Holzworth and Meng, 1984).

Notice that flows resembling viscous-like interaction (i.e. apparently into the polar cap throughout the dayside) are produced whenever an adiaroic polar cap boundary moves poleward. Examples are on both the dawn and dusk flank for the contracting polar cap (Fig. 3b) and for the anti-sunward moving cap (Fig. 3c), and on the dawn flank of the duskward moving cap (Fig. 3d) (conversely this would be on the dusk flank for a dawnward-moving cap).

Heppner and Maynard test the passes used in compiling their model to ensure that the sum of the two trans-auroral voltages for each pass equals the trans-polar voltage. They infer the convection pattern is in steady state if this condition is met. However, this condition is also met for each of the non-steady-state flow snapshots shown in Fig. 3 (because the ionospheric flow is incompressible). In real data, deviations from this condition due to polar cap expansions and contractions will be small because the time constant for the change (of order an hour) is longer than the transit time of the satellite over the pattern (typically less than 15 min). Translational polar cap motions of constant velocity during the pass also introduce only small deviations from this condition. We conclude that the departures from steady state shown in Fig. 3 are unlikely to be exposed by this test used by Heppner and Maynard. Hence it is not clear how many passes for non-steady conditions were included in the Heppner and Maynard model, or indeed any other model, and what influence these may have had on the flow patterns derived.

In order to establish the relative importance of these departures from steady state, we consider some magnitudes of the resulting potential drops for the 4-h segments of adiaroic polar cap boundary discussed earlier. If there was a major substorm, Φ_n may exceed Φ_d by something of the order of 100 kV, giving a rapid contraction of the polar cap (Clauer *et al.*, 1989). Likewise, following a strong southward turning of the IMF Φ_d could exceed Φ_n by of order 100 kV, giving a

rapid expansion of the polar cap (Lockwood *et al.*, 1986a,b). If the polar cap remained circular, these voltage differences would be distributed uniformly around the polar cap and a total voltage of 50 kV would appear between dawn and dusk, of which $\Delta_m = \Delta_a = \pm 17$ kV is across the 4-h morning and afternoon segments of adiaroic boundary. (As defined, both Δ_m and Δ_a would be positive for a polar cap contraction and negative for a polar cap expansion.) For the translational motions, the voltage is distributed sinusoidally around the polar cap boundary. The peak drop across the polar cap is $2vBr$, where v is the polar cap velocity, B is the ionospheric magnetic field and r is the polar cap radius. If we consider that the polar cap can shift by 1° of invariant latitude in, say 15 min, this is a speed of $v \approx 130 \text{ m s}^{-1}$ and for a polar cap radius of 2500 km, this corresponds to a total voltage of $2vBr = 32$ kV. For anti-sunward motion at this speed $\Delta_m = \Delta_a = vBr(1 - \cos(60^\circ)) = 8$ kV. However for duskward motion of the cap at the same speed $\Delta_m = vBr \sin(60^\circ) = 14$ kV and $\Delta_a = -14$ kV: the signs of these voltages are reversed if the motion is dawnward. Notice longer/shorter time scales for the polar cap motion will decrease/increase these estimates correspondingly.

The equivalent transpolar voltage for polar cap contraction and anti-sunward polar cap motion are comparable with, or greater than, estimates of the residual cross-cap potential when the IMF is northward, which is usually the voltage ascribed to viscous-like interactions [see reviews by Cowley (1984) and Reiff and Luhmann (1986)]. We conclude that individual cases of observations of apparently viscous-like flows in the ionosphere could result solely from polar cap contraction or translation. In general, we would expect expansion/contraction and translational movements to occur simultaneously, and in addition the polar cap will change in shape.

EFFECTS OF BINNING FLOW DATA

In all of the cases of non-steady conditions illustrated in Fig. 3, there can be no effect on long time scales, as otherwise unrealistic situations arise: polar cap expansion (a) would result in the polar caps covering the entire Earth; contraction (b) would result in the polar caps disappearing; and translations (c) and (d) would cause the polar caps to migrate to the equator. Hence the above effects could explain individual cases, but should average out in studies which take the mean of sufficient satellite passes and/or radar scans. The appearance of flows into the dayside polar cap over a wide range of M.L.T. (and not just in a restricted throat region) in average models (as

opposed to the instantaneous snapshots discussed in the previous section) could therefore be taken as evidence for the importance of the viscous-like interactions—although uncertainties about the distribution of lengths of the magnetopause reconnection X -line and about the field line mapping cannot be eliminated.

To illustrate the effects of unbiased averaging, consider the polar cap expansion and contraction shown in Figs 3a and b, respectively. When averaged over sufficiently long a period, the polar cap radius does not vary, therefore the electric field along adiaroic segments of the cap boundary must average to zero. A correctly weighted combination of Figs 3a and 3b would therefore be expected to give an average flow pattern of the form given by the Heelis *et al.* model (Fig. 1b), with restricted regions of flow into and out of the polar cap (the merging gaps), separated by shear flow reversals. Because Φ_n must equal Φ_s for such averaging, the model is inherently steady state. The same argument applies to the effects of translational movements and shape changes in the polar cap.

However, an important condition for this to be true is that the averaging represents all phases of the cycle of polar cap expansion and contraction (or movement) with the correct weight. One could envisage that any sampling will introduce biases, and indeed the data are usually selected and binned in a certain way which will introduce biases. We now consider some examples of ways in which spurious flow features may have been introduced into models by such effects. Estimates of the likely contributions to Φ_{pe} , Δ_m and Δ_a are summarized in Table 2.

(1) Data are often binned according to the three-hourly planetary magnetic index, K_p (Holt *et al.*, 1987). This index is derived from the range of magnetic variations at a network of mid-latitude stations. In general, we do not know how K_p relates to the cycles of polar cap expansion and contraction which we discussed earlier. However, it is possible that at higher K_p levels there will be a larger number of observations during the expansion and recovery phases of substorms and hence a tendency to include cases for which $\Phi_n > \Phi_d$ (as opposed to growth phases, where $\Phi_n < \Phi_d$). As a result, higher K_p may bias the data towards periods of polar cap contraction and this will give a viscous-like flow pattern on the dayside. This tendency would be even more marked if auroral electrojet indices like AE or AL were used to sort the data. Conversely, a low K_p bin may be biased towards growth phase (expanding polar cap) data and a throat region may be very marked, as in Fig. 3a. The spurious dawn-to-dusk viscous-like voltage in the model would

be numerically equal to the mean value (for the magnetic activity bin employed) of $0.5(\Phi_n - \Phi_d)$ for a circular polar cap, as discussed previously. This has a peak value of about 50 kV if only data for expansion phases of substorms are selected (for which $\Delta_m = \Delta_a = 17$ kV). We would expect biases to be less severe than this limit and a rough estimate of likely spurious viscous-like contributions to the transpolar voltage would be 5–10 kV ($\Delta_m = \Delta_a \approx 2\text{--}4$ kV).

(2) The importance of the Y component of the IMF in controlling the pattern of flow in the polar cap has become apparent and hence it has become standard practice to sort the flow data according to the prevailing IMF B_y (Heppner and Maynard, 1987; Friis-Christensen *et al.*, 1985; Holt *et al.*, 1987). If B_y has been stable for a long period there will be little translational movement of the polar caps as they are close to the appropriate displacement in the Y direction. However, if the B_y component has recently altered, the cap may still be readjusting to the prevailing IMF and V_y may not be zero. On average, therefore, there will be some positive/negative V_y of the polar cap in the Northern Hemisphere for negative/positive B_y . This being the case, we would expect a tendency for spurious viscous-like flows to appear in the dusk/dawn flank for positive/negative IMF B_y . To quantify the likely spurious potential in mean models, we estimate the peak polar cap displacement is 2° of latitude and the mean period between changes in sense of IMF B_y is 3 h, giving an average $|V_y|$ of 45 m s $^{-1}$. For a polar cap radius of 2500 km, this places 6 kV across each quadrant of the polar cap boundary: for duskward motion, this adds to any viscous-like voltage in the morning sector but in the afternoon sector an equal amount is subtracted from any viscous interaction potential which is actually present ($\Delta_m = 5$ kV; $\Delta_a = -5$ kV). The effect on these two sectors is reversed for the opposite polarity of B_y . Note that although this effect can alter the shape and voltage of the dawn and dusk convection cells in the mean models, no spurious viscous-like contribution is introduced into the total dawn-to-dusk transpolar voltage, Φ_{pc} .

(3) The method used by Heppner and Maynard to compile their model used pattern recognition of the distribution of potential along the satellite orbit to classify the data. Passes of a given classification were then synthesized together into a flow pattern. It should be noted that the classification procedure could, in itself, select passes for a given non-steady-state polar cap situation (for example, contracting polar cap). Such selection could generate a spurious flow across the dayside polar cap boundary, if the actual non-steady pattern is considered to be a steady state one.

Another possibility is that the orbit classification scheme could introduce a bias by selecting passes for which the magnitude of the potential on the convection boundary nearer noon is lower (even for equal representations of expanding and contracting polar cap). Were this to be the case, spurious flows into the polar cap would then be generated in the convection model. In other words, it is possible that noon–midnight passes of a given classification may, on average, be for times of lower transpolar voltage than dawn–dusk passes of the same classification.

(4) Exclusion of passes showing irregular patterns of flow/potential or non-steady-state behaviour (i.e. when the measured transpolar voltage does not equal the sum of the two transauroral voltages) may exclude certain phases of the polar cap cycle and hence bias the averaging.

IMPLICATIONS FOR ESTIMATES OF TRANSPOLAR VOLTAGE

Figure 4 shows a polar cap boundary with adiaric segments AB and CD and dayside and nightside merging gaps (DA and BC , respectively). Consider satellite passes which cut both AB and CD (as does the path XY shown). In practice such passes could be identified as ones showing nearly shear flow reversals at both the dawn and dusk flank. Typical boundary speeds for contraction, expansion and translation of the polar cap are near 100 m s $^{-1}$, and flow data near the boundaries will be dominated by the convection speeds of typically 1 km s $^{-1}$ along the boundary. As

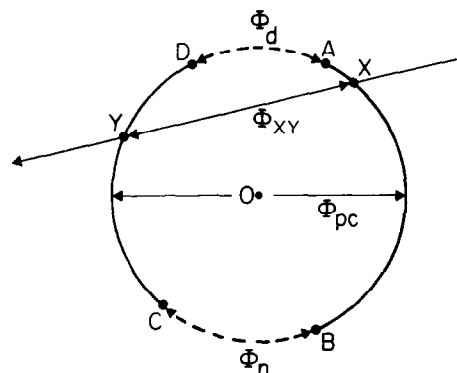


FIG. 4. OBSERVATIONS OF TRANSPOLAR VOLTAGE. The voltage measured in a satellite path XY is Φ_{xy} , which is taken to intersect both the adiaric polar cap boundary segments AB and CD . Symbols are as used in Fig. 3. The voltage across the dayside merging gap, AD , is Φ_d in the Earth's frame of reference; the corresponding value for the nightside merging gap, BC , is Φ_n . The dawn-to-dusk transpolar voltage is Φ_{pc} .

a result, it would be almost impossible to tell if the convection boundaries at X and Y are in motion or not. The transpolar voltage, Φ_{XY} is derived by integrating the electric field along the satellite track (corresponding to the flows perpendicular to the track) between X and Y (Reiff *et al.*, 1981; Doyle and Burke, 1983; Wygant *et al.*, 1983). If it is assumed that the flow pattern is in steady state (i.e. X and Y are static, $\Phi_{XY} = \Phi_d = \Phi_n = \Phi'_d = \Phi'_n$ because the merging gaps are also static) and the measured voltage is the transpolar voltage, Φ_{pc} . However, in the more general case where the polar cap is expanding/contracting the measured voltage will depend on the satellite orbit configuration, even for a fixed Φ_d and Φ_n . It can be easily shown that for any satellite path that passes through the centre of a circular polar cap, Φ_{XY} is the arithmetic mean of Φ_d and Φ_n and hence is always equal to the dawn-to-dusk voltage, Φ_{pc} .

$$\Phi_{pc} = 0.5(\Phi_d + \Phi_n). \quad (6)$$

However, if the path does not pass through the centre and/or the polar cap is not circular, Φ_{XY} can vary between Φ_d (for X at A and Y at D) and Φ_n (for X at B and Y at C). Hence expansion/contraction of the polar cap and satellite orbit configuration could greatly add to the scatter in regression analysis of Φ_{XY} measurements with IMF and solar wind parameters.

In addition, during periods of northward IMF ($\Phi_d \approx 0$) residual reconnection in the tail ($\Phi_n > 0$) can contribute to Φ_{XY} : in the past, this voltage for northward IMF has often been attributed entirely to viscous-like interaction at the magnetopause. Wygant *et al.* (1983) found a spread in transpolar voltages 1 h after northward turnings of the IMF of between 10 and 100 kV: 8 h later values had fallen to below about 15 kV. The spread shortly after the northward turning would be due to different orbit paths (higher residual values being for nightside passes) and the decrease of the larger values reflects the decay of the nightside reconnection rate. Hence, on the basis of these data we would estimate that only 15 kV of the residual voltage during northward IMF is due to viscous-like interaction and the remainder (up to about 85 kV, decaying away over about 8 h) is due to continuing reconnection in the tail.

DISCUSSION AND CONCLUSIONS

Tables 1 and 2 summarize the estimates given in this paper of various contributions to the voltages Δ_m and Δ_a and the transpolar voltage, Φ_{pc} . These estimates are based on estimates of various other parameters (e.g. polar cap radius, reconnection rates, mean delay between polarity reversal in IMF B_y , etc.)

TABLE 1. TYPICAL CONTRIBUTIONS TO VOLTAGES ALONG CONVECTION BOUNDARY IN SNAPSHOTS OF FLOW PATTERNS

Polar cap effect	Δ_m (kV)	Δ_a (kV)	$\Delta_m + \Delta_a$ (kV)	Φ_{pc} (kV)
Contraction	17	17	34	50
Anti-sunward motion	8	8	16	32
Duskward motion	14	-14	0	0
Dawnward motion	-14	14	0	0

TABLE 2. TYPICAL CONTRIBUTIONS TO VOLTAGES ALONG CONVECTION BOUNDARY IN AVERAGE FLOW PATTERNS

Polar cap effect	Δ_m (kV)	Δ_a (kV)	$\Delta_m + \Delta_a$ (kV)	Φ_{pc} (kV)
Variability of latitude of dayside merging gap	13	13	26	26
Variability of M.L.T. of merging gap	10	10	20	0
Bias toward contraction	3	3	6	8
Selection of IMF B_y	± 5	$\pm (-5)$	0	0

and the reader is referred to the main body of the text for the details of the values used.

Table 1 summarizes some ways in which apparently viscous-like flows into the dayside polar cap can be generated in instantaneous flow measurements by departures from steady state. It can be seen that polar cap contraction is the largest effect which can account for any typical viscous-like voltage, as can anti-sunward motion of the entire polar cap. The dawn/dusk motion can introduce a strong asymmetry between the dawn and dusk cell boundaries but does not contribute to the transpolar voltage.

The conclusion is that instantaneous observations of rotational flows into the polar cap are not necessarily an indicator of viscous-like interaction, even if they occur well away from the predicted location of the reconnection merging gap. Considerable scatter in satellite observations of transpolar voltage (which assume steady state) will be introduced by departures from steady state, if orbits which do not pass through the centre of a circular polar cap are used. Note that orbits for which the satellite does pass close to the cap centre will be rather rare.

The corresponding effects in average flow models are difficult to estimate, because they will depend on biasing of the data by the classification scheme and the activity/IMF binning employed. In Table 2 we estimate that there will be some dawn-dusk asymmetry introduced by non-steady-state conditions and binning the data according to IMF B_y , but this is only

about a third of the possible effect in instantaneous flow data. Similarly, we estimate a bias favouring selection of data for a contracting polar cap may add up to about 8 kV to Φ_{pc} , only $(\Delta_m + \Delta_a) = 6$ kV of which appears across the dayside shear flow boundaries of the Heelis *et al.* model.

Considering the differences between the Heelis *et al.* and Heppner and Maynard models we find a difference in $(\Delta_m + \Delta_a)$ of 44 kV for the 06:00–10:00 and 14:00–18:00 M.L.T. segments of the convection boundary. Hence the above estimate of the effect of any bias to contracting polar cap does not appear to be adequate to explain this difference between these two models. In fact, for this explanation the actual Φ_n would have to exceed Φ_d by nearly 130 kV on average (for a circular polar cap). The effect of variability of the dayside convection boundary latitude is likewise not an explanation of this difference, because Heppner and Maynard have averaged the data in the correct way to avoid such effects. Variability of the M.L.T. of the ends of the merging gap is a possible explanation of a large part of the difference (see Table 2).

The dawn–dusk asymmetry in the difference between the two models could be explained by the effects of dusk-/dawnwards polar cap motions. In the Heppner and Maynard model, $|\Delta_m - \Delta_a|$ is of order 4 kV, whereas Table 2 gives an estimate that as much as 10 kV could be caused by non-steady-state effects.

Note that one or more of the above listed effects could act while viscous-like interaction also contributed to Δ_m and Δ_a and hence Φ_{pc} . None appear to be large enough to eliminate viscous-like interaction as a cause of any of the differences between the Heelis and Heppner *et al.* models. Neither are the values given in Table 2 large enough to explain on their own the $(\Delta_m + \Delta_a)$ of about 37 kV, derived from the sinusoidal fits to the distribution of potential along the boundary by Lu *et al.* (1989). These authors suggest some of the differences between their results and those of Heppner and Maynard are due to the choice of reversal, when multiple reversals are present. Lu *et al.* used the reversal closest to the precipitation boundary (thought to be the open/closed field line boundary) and found single reversals were only present in about a third of cases. It is suggested here that at least some of the difference between the Heppner and Maynard and Lu flow patterns could also be due to the classification and binning of the data. The results of Lu *et al.* could be explained by instantaneous flow patterns of the kind given by the Heelis *et al.* model with variability in the M.L.T. of the dayside merging gap, or by the departures from steady state shown in Fig. 3, with some contribution from viscous-like interaction outside the merging gap.

It is well known that great care must be taken when averaging flow/electric field data. If data for a given location are averaged, Table 2 shows that variability in the latitude of the dayside polar cap boundary can introduce large spurious voltages and spurious rotational reversals into the flow pattern, in addition to those caused by variability in the M.L.T. of the merging gap. This sort of averaging was used, for example, by Oliver *et al.* (1983), Holt *et al.* (1987) and Etemadi *et al.* (1988). Due to insufficient latitudinal coverage of the radar data, none of these models actually covered much of the convection boundary region and hence this effect was not a major problem. In the Heppner and Maynard (1987) model, this effect was avoided by averaging boundary location and peak potential separately. However, other variations, for example in the M.L.T. of the merging gap, could introduce apparent rotational reversals into all average convection models which are not present in instantaneous flow snapshots. Departures from steady state do affect the instantaneous flow patterns and, as a result, subtle changes in average patterns may result from classification of data or the IMF/activity bins used to average the data.

The transpolar voltage and the convection pattern depend upon the rates of reconnection at the magnetopause and in the geomagnetic tail and upon the viscous-like interaction across the magnetopause flanks. Only with proper analysis of the two reconnection voltages (as done for example by Holzer *et al.*, 1986) can the true residual voltage which is attributed to other mechanisms (i.e. viscous-like interaction) be quantified. Much, but not all, of the viscous-like voltage could result from departures from steady state. With proper analysis of merging rate imbalances, ionospheric flow observations and models could be used to quantify the two major momentum transfer mechanisms across the magnetopause. Uncertainties in field line mapping mean that the precise locations on the magnetopause of these processes will not, however, be known.

When considering the validity of current models, one must bear in mind the application. In this paper, we have attempted to outline some problems with the various methods used to compile the models, rather than investigate all problems with all models and all their implications. However, it should be noted that convection models have been, and will continue to be, of great importance but would be improved by allowance for departures from steady state.

First-order allowance for non-steady conditions could be made by characterizing the flow pattern with just one additional parameter. Allowance for an imbalance in reconnection rates (polar cap expan-

sion/contraction), requires the model to use inputs quantifying dayside and nightside reconnection rates separately. This could be done directly, for example using some function of the IMF B_z component and solar wind speed and a function of an auroral electroject index (to quantify Φ_d and Φ_n , respectively), as done by Holzer *et al.* (1986). Using one or other of these alone assumes steady state and is an inherently inadequate description. Alternatively, an equivalent description could use the dawn-to-dusk voltage Φ_{pc} and the rate of change of the polar cap area. The latter could be monitored using global auroral imagers or possibly a global magnetometer network. From Faraday's Law (5) and the definition of Φ_{pc} (6), we find for a circular polar cap:

$$\Phi_d = \Phi_{pc} + (1-f)B(dA/dt)/2 \quad (7)$$

$$\Phi_n = \Phi_{pc} - (1-f)B(dA/dt)/2. \quad (8)$$

Hence knowledge of the rate of change of polar cap area, along with the known regressions of Φ_{pc} with IMF components and solar wind speed, could be used to quantify Φ_d and Φ_n . In fact, knowledge of any two of the four parameters, Φ_{pc} , Φ_d , Φ_n and (dA/dt) is all that is required. (This assumes a circular polar cap and that the fraction f is known, as currently required as an input for the Heelis *et al.* model.)

In addition, the history of the IMF B_y component, and not just the prevailing value, should ideally be accounted for. These changes would result in considerable increases in complexity of the models which would also require more input information before they could be applied. Hence the requirement for models which do assume steady state is likely to persist. This is valuable provided it is remembered that detailed features, for example the nature of the flow reversals and the transpolar voltage, will be influenced by this assumption and this may have implications for the application in question.

REFERENCES

- Beaujardiere, O. de la, Evans, D. S., Kamide, Y. and Lepping, R. P. (1987) Response of the auroral oval precipitation and magnetospheric convection to changes in the interplanetary magnetic field. *Ann. Geophys.* **5A**, 518.
- Burch, J. L. (1973) Rate of erosion of dayside magnetic flux based on a quantitative study of the dependence of polar cap latitude on the interplanetary magnetic field. *Radio Sci.* **8**, 955.
- Burch, J. L., Reiff, P. H., Menietti, J. D., Heelis, R. A., Hanson, W. B., Shawhan, S. D., Shelley, E. G., Suguira, M., Weimer, D. R. and Winningham, J. D. (1985) IMF B_z -dependent plasma flow and Birkeland currents in the dayside magnetosphere: 1. *Dynamics Explorer* observations. *J. geophys. Res.* **90**, 1577.
- Clauer, C. R., Kelly, J. D., Lockwood, M., Robinson, R. M., Rouhoniemi, J. M., Beaujardiere, O. de la and Hakkinen, L. (1989) June 1987 GISMOS experiment: preliminary report on high-time resolution, multi-radar measurements. *Adv. Space Res.* **9**, 29.
- Cowley, S. W. H. (1981) Magnetospheric asymmetries associated with the Y -component of the IMF. *Planet. Space Sci.* **29**, 79.
- Cowley, S. W. H. (1984) Solar wind control of magnetospheric convection, in *Achievements of the International Magnetospheric Study IMS*, p. 483. ESA SP-217, ESTEC, Noordwijk, The Netherlands.
- Cowley, S. W. H., Morelli, J. P. and Lockwood, M. (1991) Displacements of the polar cusp and polar cap related to the X and Y components of the IMF. *J. geophys. Res.* (in press).
- Doyle, M. A. and Burke, W. J. (1983) S3-2 measurements of polar cap potential. *J. geophys. Res.* **88**, 9125.
- Etemadi, A., Cowley, S. W. H., Lockwood, M., Bromage, B. J. I., Willis, D. M. and Lühr, H. (1988) The dependence of high-latitude dayside ionospheric flows on the north-south component of the IMF: a high time resolution correlation analysis using *EISCAT "POLAR"* and *AMPTE UKS* and *IRM* data. *Planet. Space Sci.* **36**, 471.
- Foster, J. C. (1983) An empirical electric field model derived from Chatanika radar data. *J. geophys. Res.* **88**, 981.
- Foster, J. C., Turunen, T., Pollari, P., Kohl, H. and Wickwar, V. B. (1989) Multi-radar mapping of auroral convection. *Adv. Space Res.* **9**, 19.
- Freeman, M. P. and Southwood, D. J. (1988) The effects of magnetospheric erosion on mid- and high-latitude ionospheric flows. *Planet. Space Sci.* **36**, 509.
- Friis-Christensen, E., Kamide, Y., Richmond, A. D. and Matsushita, S. (1985) Interplanetary magnetic field control of high-latitude ionospheric fields and currents determined from Greenland magnetometer data. *J. geophys. Res.* **90**, 1325.
- Hairston, M. R. and Heelis, R. A. (1990) Model of the high-latitude ionospheric convection pattern during southward Interplanetary Magnetic Field using *DE 2* data. *J. geophys. Res.* **95**, 2333.
- Hapgood, M. A., Willis, D. M., Lockwood, M., Bowe, G. A. and Tulunay, Y. K. (1991) Variability of the interplanetary medium at 1 A.U. over 24 years: 1963–1986. *Planet. Space Sci.* **39**, 411.
- Heelis, R. A. (1984) The effects of interplanetary magnetic field orientation on dayside high-latitude convection. *J. geophys. Res.* **89**, 2873.
- Heelis, R. A. and Hanson, W. B. (1980) High-latitude ion convection in the nightside F -region. *J. geophys. Res.* **85**, 1995.
- Heelis, R. A., Hanson, W. B. and Burch, J. L. (1976) Ion convection reversals in the dayside cleft. *J. geophys. Res.* **81**, 3803.
- Heelis, R. A., Lowell, J. K. and Spiro, R. W. (1982) A model of the high-latitude ionospheric convection pattern. *J. geophys. Res.* **87**, 6339.
- Heppner, J. P. (1972) Polar cap electric field distributions related to the interplanetary magnetic field direction. *J. geophys. Res.* **77**, 4877.
- Heppner, J. P. (1973) High latitude electric fields and their modulations related to interplanetary magnetic field parameters. *Radio Sci.* **8**, 933.
- Heppner, J. P. (1977) Empirical models of high-latitude electric fields. *J. geophys. Res.* **82**, 1115.
- Heppner, J. P. and Maynard, N. C. (1987) Empirical high-latitude electric field models. *J. geophys. Res.* **92**, 4467.

- Holt, J. M., Wand, R. H., Evans, J. V. and Oliver, W. L. (1987) Empirical models for the plasma convection at high latitudes from Millstone Hill observations. *J. geophys. Res.* **92**, 203.
- Holzer, R. E., McPherron, R. L. and Hardy, D. A. (1986) A quantitative model of the magnetospheric flux transfer process. *J. geophys. Res.* **91**, 3287.
- Holzworth, R. H. and Meng, C.-I. (1984) Auroral boundary variations and the interplanetary magnetic field. *Planet. Space Sci.* **32**, 25.
- Hones, E. W., Jr. (1985) The poleward leap of the auroral electrojets as seen in auroral images. *J. geophys. Res.* **90**, 5333.
- Jørgensen, T. S., Friis-Christensen, E., Wickwar, V. B., Kelly, J. D., Clauer, C. R. and Banks, P. M. (1984) On the reversal from "sunward" to "antisunward" plasma convection in the dayside high latitude ionosphere. *Geophys. Res. Lett.* **1**, 887.
- Lockwood, M., Cowley, S. W. H. and Freeman, M. P. (1990) The excitation of plasma convection in the high latitude ionosphere. *J. geophys. Res.* **95**, 7961.
- Lockwood, M., Cowley, S. W. H., Todd, H., Willis, D. M. and Clauer, C. R. (1988) Ion flows and heating at a contracting polar cap boundary. *Planet. Space Sci.* **36**, 1229.
- Lockwood, M., Eyken, A. P. van, Bromage, B. J. I., Waite, J. H., Jr., Moore, T. E. and Doupnik, J. R. (1986b) Low-energy ion outflows from the ionosphere during a major cap expansion—evidence for equatorward motion of inverted-V structures. *Adv. Space Res.* **6**, 93.
- Lockwood, M., Eyken, A. P. van, Bromage, B. J. I., Willis, D. M. and Cowley, S. W. H. (1986a) Eastward propagation of a plasma convection enhancement following a southward turning of the interplanetary magnetic field. *Geophys. Res. Lett.* **13**, 72.
- Lockwood, M. and Freeman, M. P. (1989) Recent ionospheric observations relating to solar wind-magnetosphere coupling. *Phil. Trans. R. Soc. A* **328**, 93.
- Lockwood, M., Quegan, S. and Fuller-Rowell, T. J. (1991) On the implications of variations in plasma convection for modelling the high-latitude ionosphere and thermosphere. *Planet. Space Sci.* (to be submitted).
- Lu, G., Reiff, P. H., Hairston, M. R., Heelis, R. A. and Karty, J. L. (1989) Distribution of convection potential around the polar cap boundary as a function of interplanetary magnetic field. *J. geophys. Res.* **94**, 13,447.
- Meng, C.-I. (1980) Polar cap variations and the interplanetary magnetic field, in *Dynamics of the Magnetosphere* (Edited by Akasofu, S.-I.), p. 23. D. Reidel, Dordrecht.
- Moses, J. J., Siscoe, G. L., Heelis, R. A. and Winningham, J. D. (1989) Polar cap deflation during magnetospheric substorms. *J. geophys. Res.* **94**, 3785.
- Mozer, F. S. (1984) Electric field evidence for viscous interaction at the magnetopause. *Geophys. Res. Lett.* **11**, 981.
- Mozer, F. S., Gonzales, W. D., Bogott, F., Kelley, M. C. and Shutz, S. (1974) High-latitude electric fields and the three-dimensional interaction between the interplanetary and terrestrial magnetic fields. *J. geophys. Res.* **79**, 56.
- Newell, P. T. and Meng, C.-I. (1989) On quantifying the distinctions between the cusp and the cleft LLBL, in *Electromagnetic Coupling in the Polar Clefts and Caps* (Edited by Sandholt, P. E. and Egeland, A.), p. 87. NATO ASI series C, Vol. 278. Kluwer Academic, Dordrecht.
- Oliver, W. L., Holt, J. M., Wand, R. H. and Evans, J. V. (1983) Millstone Hill incoherent scatter observations of auroral convection over $60^\circ < \Lambda < 75^\circ$: 3. Average patterns versus *Kp*. *J. geophys. Res.* **88**, 5505.
- Rees, D. and Fuller-Rowell, T. J. (1989) Geomagnetic response of the polar thermosphere and ionosphere, in *Electromagnetic Coupling in the Polar Clefts and Caps* (Edited by Sandholt, P. E. and Egeland, A.), p. 355. NATO ASI series C, Vol. 278. Kluwer Academic, Dordrecht.
- Reiff, P. H., Burch, J. L. and Heelis, R. A. (1978) Dayside auroral arcs and convection. *Geophys. Res. Lett.* **5**, 391.
- Reiff, P. H., Hill, T. W. and Burch, J. L. (1977) Solar wind plasma injection at the dayside magnetospheric cusp. *J. geophys. Res.* **82**, 479.
- Reiff, P. H. and Luhmann, J. G. (1986) Solar wind control of the polar cap voltage, in *Solar Wind-Magnetosphere Coupling* (Edited by Kamide, Y. and Slavin, J. A.), p. 452. Terra Scientifica, Tokyo.
- Reiff, P. H., Spiro, R. W. and Hill, T. W. (1981) Dependence of polar cap potential drop on interplanetary parameters. *J. geophys. Res.* **86**, 7639.
- Rich, F. J. and Maynard, N. C. (1989) Consequences of using simple analytic functions for the high-latitude convection electric field. *J. geophys. Res.* **94**, 3687.
- Richmond, A. D., Kamide, Y., Ahn, B.-H., Akasofu, S.-I., Alcayde, D., Blanc, M., Beaujardiere, O. de la, Evans, D. S., Foster, J. C., Friis-Christensen, E., Fuller-Rowell, T. J., Holt, J. M., Knipp, D., Kroehl, H. W., Lepping, R. P., Pellinen, R. J., Senior, C. and Zaitzev, A. N. (1988) Mapping electrodynamic features of the high-latitude ionosphere from localised observations: combined incoherent-scatter radar and magnetometer measurements from 18–19 January, 1984. *J. geophys. Res.* **93**, 5760.
- Rostoker, G., Savoie, D. and Phan, T. D. (1988) Response of magnetosphere-ionosphere current systems to changes in the interplanetary magnetic field. *J. geophys. Res.* **93**, 8633.
- Siscoe, G. L. and Huang, T. S. (1985) Polar cap inflation and deflation. *J. geophys. Res.* **90**, 543.
- Sojka, J. J. (1989) Global scale, physical models of the *F*-region ionosphere. *Rev. Geophys.* **27**, 371.
- Southwood, D. J. (1985) Theoretical aspects of ionosphere-magnetosphere-solar wind coupling. *Adv. Space Res.* **5**, 7.
- Southwood, D. J. (1987) The ionosphere signatures of flux transfer events. *J. geophys. Res.* **92**, 3207.
- Todd, H., Cowley, S. W. H., Etemadi, A., Bromage, B. J. I., Lockwood, M., Willis, D. M. and Lühr, H. (1988) Flow in the high-latitude ionosphere: measurements at 15-second resolution made using the *EISCAT* "POLAR" experiment. *J. atmos. terr. Phys.* **50**, 423.
- Volland, H. (1978) A model of the magnetospheric electric convection field. *J. geophys. Res.* **83**, 2695.
- Wygant, J. R., Torbert, R. B. and Mozer, F. S. (1983) Comparison of *S3-2* polar cap potential drops with the interplanetary magnetic field and models of magnetopause reconnection. *J. geophys. Res.* **88**, 5727.